Tetranuclear Cr-Ln ferrocenecarboxylate complexes with a defect-dicubane structure: synthesis, magnetism, and thermolysis

Pavel S. Koroteev,[a]* Zhanna V. Dobrokhotova,[a] Andrey B. Ilyukhin,[a] Ekaterina V. Belova,[a,b] Alexey D. Yapryntsev,[a] Mathieu Rouzières,[c] Rodolphe Clérac,[c]* Nikolay N. Efimov.[a]

[a] *N.S. Kurnakov Institute of General and Inorganic Chemistry, Russian Academy of Sciences, Leninsky prosp. 31, 119991 Moscow, GSP-1, Russian Federation*

[b] *Lomonosov Moscow State University, Department of Chemistry, GSP-1, Leninskie Gory 1/3, 119991 Moscow, Russian Federation*

[c] *Univ. Bordeaux, CNRS, Centre de Recherche Paul Pascal, UMR 5031, 33600 Pessac, France*

Correspondence: pskoroteev@list.ru, clerac@crpp-bordeaux.cnrs.fr

SUPPLEMENTARY MATERIALS

Table S1. Crystal data and structure refinement for **1 – 5** and **1a**.

Identification code	**1**	**2**	**3**	**4**	**5**
Empirical formula	$C_{78}H_{96}Cr_2Fe_4N_4O_{24}Tb_2$	$C_{78}H_{96}Cr_2Dy_2Fe_4N_4O_{24}$	$C_{78}H_{96}Cr_2Fe_4Ho_2N_4O_{24}$	$C_{78}H_{96}Cr_2Er_2Fe_4N_4O_{24}$	$C_{78}H_{96}Cr_2Fe_4N_4O_{24}Y_2$
Formula weight	2118.82	2125.98	2130.84	2135.50	1978.80
Temperature, K	150(2)	150(2)	150(2)	150(2)	150(2)
Wavelength, Å	0.71073	0.71073	0.71073	0.71073	0.71073
Crystal system	Monoclinic	Monoclinic	Monoclinic	Monoclinic	Monoclinic
Space group	$P2_1/n$	$P2_1/n$	$P2_1/n$	$P2_1/n$	$P2_1/n$
a, Å	15.0231(4)	15.2812(4)	15.2579(5)	14.9585(4)	15.0033(5)
b, Å	17.2324(5)	16.7770(5)	16.7324(5)	17.2006(5)	17.1273(5)
c, Å	15.6619(4)	15.8983(5)	15.9113(5)	15.6650(5)	15.6663(5)
β, °	99.7370(10)	103.1360(10)	103.0660(10)	99.7280(10)	100.1480(10)
Volume, Å^3	3996.21(19)	3969.2(2)	3957.0(2)	3972.6(2)	3962.7(2)
Z	2	2	2	2	2
D (calc), Mg/m^3	1.761	1.779	1.788	1.785	1.658
μ, mm^{-1}	2.789	2.909	3.029	3.138	2.500
F(000)	2132	2136	2140	2144	2028
Crystal size, mm	0.3 × 0.3 × 0.2	0.4 × 0.3 × 0.28	0.24 × 0.24 × 0.16	0.2 × 0.2 × 0.2	0.32 × 0.3 × 0.12
θ range, °	2.101, 29.603	2.064, 30.544	2.067, 28.715	2.106, 30.046	2.102, 29.180
Index ranges	$-20 \le h \le 20$	$-21 \le h \le 21$	$-19 \le h \le 20$	$-21 \le h \le 20$	$-19 \le h \le 20$
	$-23 \le k \le 23$	$-23 \le k \le 23$	$-22 \le k \le 22$	$-24 \le k \le 23$	$-22 \le k \le 22$
	$-21 \le l \le 21$	$-22 \le l \le 22$	$-21 \le l \le 21$	$-21 \le l \le 22$	$-21 \le l \le 20$
Reflections collected	53330	55260	50647	54182	50517
Independent reflections, R_{int}	11218, 0.0515	12036, 0.0376	10141, 0.0469	11600, 0.0487	10360, 0.0525
Completeness to θ = 25.242°	99.9 %	100.0 %	100.0 %	99.9 %	99.9 %
Absorption correction	Semi-empirical from equivalents	Semi-empirical from equivalents	Semi-empirical from equivalents	Semi-empirical from equivalents	Semi-empirical from equivalents
Max., min. transmission	0.7459, 0.6117	0.7461, 0.5241	0.7458, 0.5678	0.746, 0.607	0.7458, 0.556
Refinement method	Full-matrix least-squares on F^2	Full-matrix least-squares on F^2	Full-matrix least-squares on F^2	Full-matrix least-squares on F^2	Full-matrix least-squares on F^2
Data / restraints / parameters	11218 / 0 / 595	12036 / 15 / 595	10141 / 15 / 594	11600 / 0 / 595	10360 / 0 / 595
Goodness-of-fit	0.974	0.999	0.974	0.923	1.068
R_1, wR_2 [$I > 2\sigma(I)$]	0.0335, 0.0788	0.0316, 0.0814	0.0302, 0.0709	0.0309, 0.0722	0.0381, 0.0824
R_1, wR_2 (all data)	0.0563, 0.0932	0.0444, 0.0928	0.0443, 0.0785	0.0518, 0.0842	0.0800, 0.0971
Largest diff. peak and hole, e.Å^{-3}	1.273, -0.618	1.624, -1.059	1.039, -0.687	1.302, -0.690	0.598, -0.513

Identification code	**1a**
Empirical formula	$C_{78}H_{96}Cr_2Fe_4N_4O_{24}Tb_2$
Formula weight	2118.82
Temperature, K	150(2)
Wavelength, Å	0.71073
Crystal system	Triclinic
Space group	P-1
a, Å	10.0901(18)
b, Å	12.780(3)
c, Å	16.698(3)
α, °	105.437(6)
β, °	96.248(6)
γ, °	95.977(6)
Volume, Å^3	2043.2(7)
Z	1
D (calc), Mg/m^3	1.722
μ, mm^{-1}	2.728
F(000)	1066
Crystal size, mm	0.08 × 0.08 × 0.02
θ range, °	2.371, 25.349
Index ranges	$-12 \leq h \leq 12$ $-15 \leq k \leq 15$ $-20 \leq l \leq 20$
Reflections collected	26431
Independent reflections, R_{int}	7475, 0.1715
Completeness to $\theta = 25.242°$	99.9 %
Absorption correction	Semi-empirical from equivalents
Max,. min. transmission	0.0439, 0.0223
Refinement method	Full-matrix least-squares on F^2
Data / restraints / parameters	7475 / 0 / 478
Goodness-of-fit	0.946
R_1, wR_2 [$I > 2\sigma(I)$]	0.0691, 0.1290
R_1, wR_2 (all data)	0.1693, 0.1655
Largest diff. peak and hole, e.Å^{-3}	1.601, -1.928

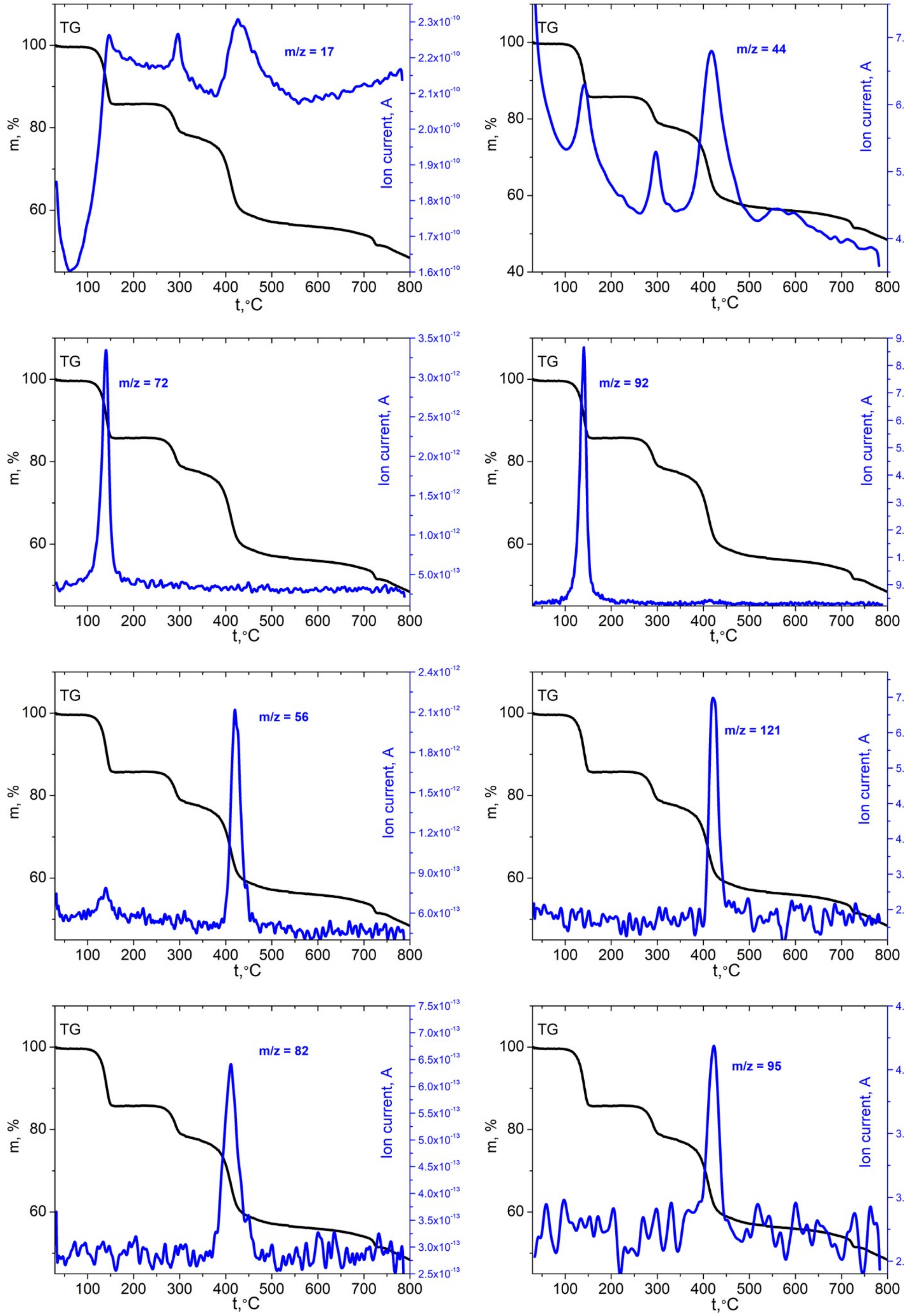

Fig. S1. Ionic currents in the mass spectrum of the gases evolved during thermolysis of Ho complex **3** under argon.

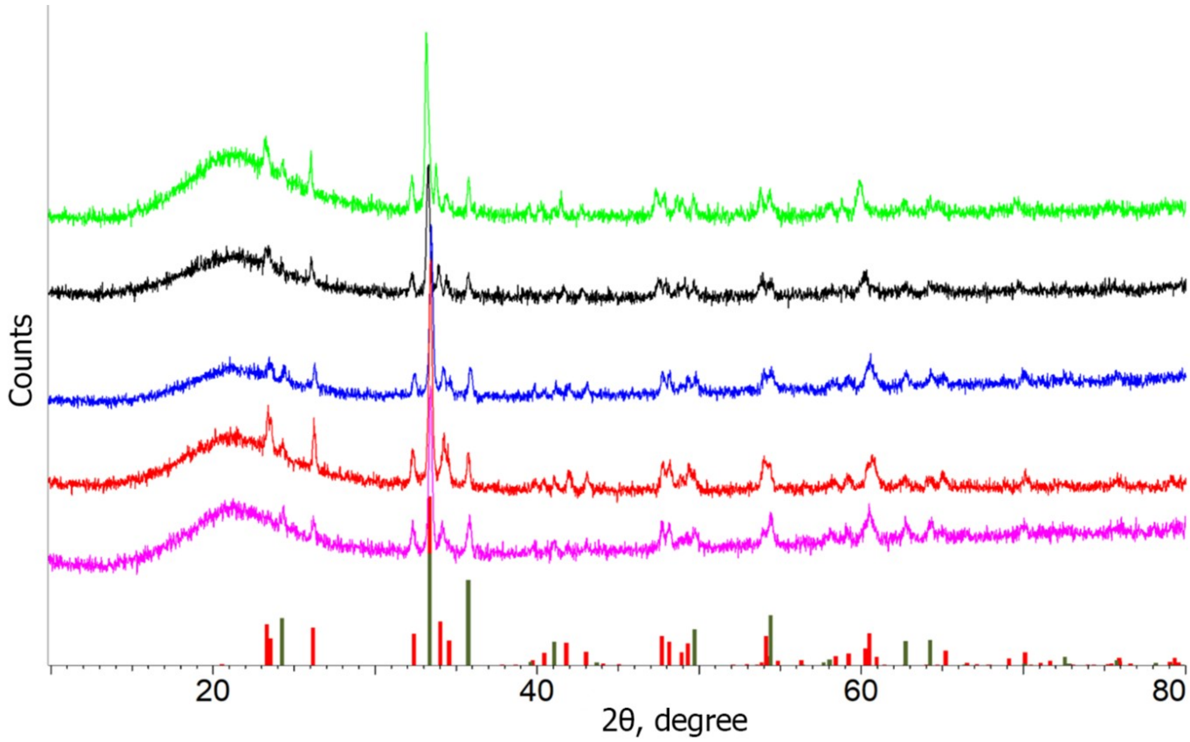

Fig. S2. Powder X-ray diffraction patterns of solid oxidative thermolysis products from complexes **1** (**green** line), **2** (**black** line), **3** (**blue** line), **4** (**red** line), and **5** (**magenta** line). Vertical sticks represent the X-ray diffraction patterns of $DyCrO_3$ (**red** sticks), and $Cr_{0.75}Fe_{1.25}O_3$ (**brown** sticks; taken from COD/PDF database, numbers COD 1008154 and PDF 01-077-9861, respectively).

Table S2a (*see caption below*).

Spectrum	Cr	Fe	Tb
Spectrum 1	22.35	55.73	21.93
Spectrum 2	21.35	55.99	22.65
Spectrum 3	21.26	55.93	22.81
Spectrum 4	21.23	55.90	22.87
Spectrum 5	21.34	56.02	22.64
Spectrum 6	21.28	55.84	22.88
Mean	21.47	55.90	22.63

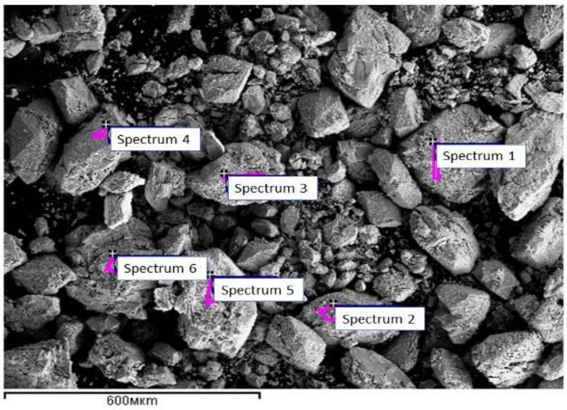

Fig. S3a (*see caption below*).

Table S2b.

Spectrum	Cr	Fe	Dy
Spectrum 1	25.02	51.18	23.80
Spectrum 2	26.17	47.93	25.90
Spectrum 3	25.16	50.59	24.25
Spectrum 4	25.02	50.84	24.14
Spectrum 5	23.06	53.44	23.50
Mean	24.75	50.98	24.27

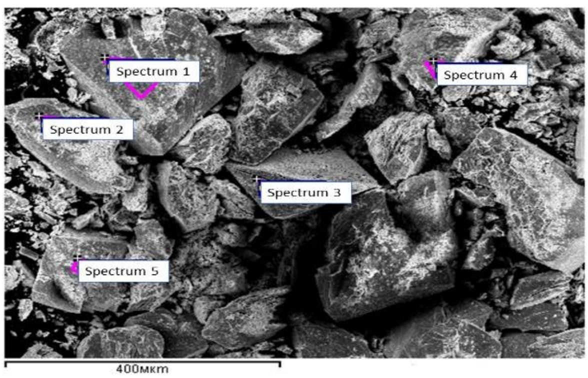

Fig. S3b.

Table S2c.

Spectrum	Cr	Fe	Ho
Spectrum 1	25.01	49.87	25.13
Spectrum 2	24.72	49.97	25.31
Spectrum 3	24.88	50.05	25.07
Spectrum 4	24.76	50.09	25.15
Spectrum 5	24.95	49.79	25.26
Mean	24.86	49.95	25.18

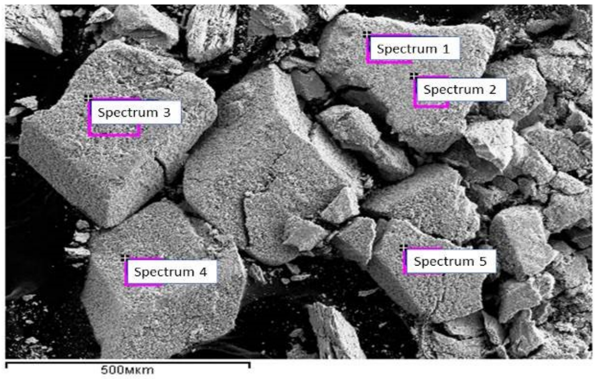

Fig. 3c.

Table S2d.

Spectrum	Cr	Fe	Er
Spectrum 1	24.58	51.05	24.37
Spectrum 2	24.53	50.50	24.97
Spectrum 3	24.29	50.74	24.97
Spectrum 4	25.44	48.02	26.54
Spectrum 5	24.64	50.81	24.55
Mean	24.70	50.21	25.09

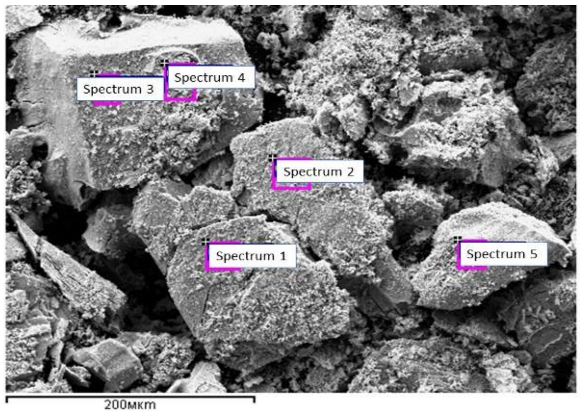

Fig. 3d.

Table S2e.

Spectrum	Cr	Fe	Y
Spectrum 1	25.30	48.00	26.70
Spectrum 2	25.95	50.06	23.99
Spectrum 3	26.35	50.00	23.65
Spectrum 4	26.12	49.91	23.97
Spectrum 5	25.97	49.93	24.11
Spectrum 6	25.99	50.01	24.01
Mean	25.95	49.65	24.40

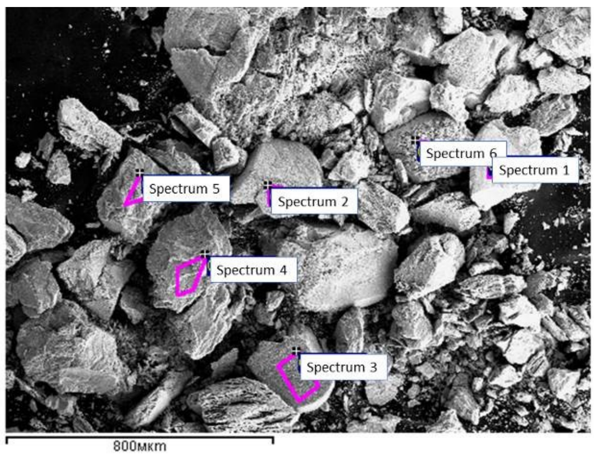

Fig. 3e.

Tables 2a-e; Figs. S3a-e. Energy dispersive X-ray microanalyses data (Tables, at.%) and corresponding SEM images for oxidative thermolysis products of complexes **1**-**5**.

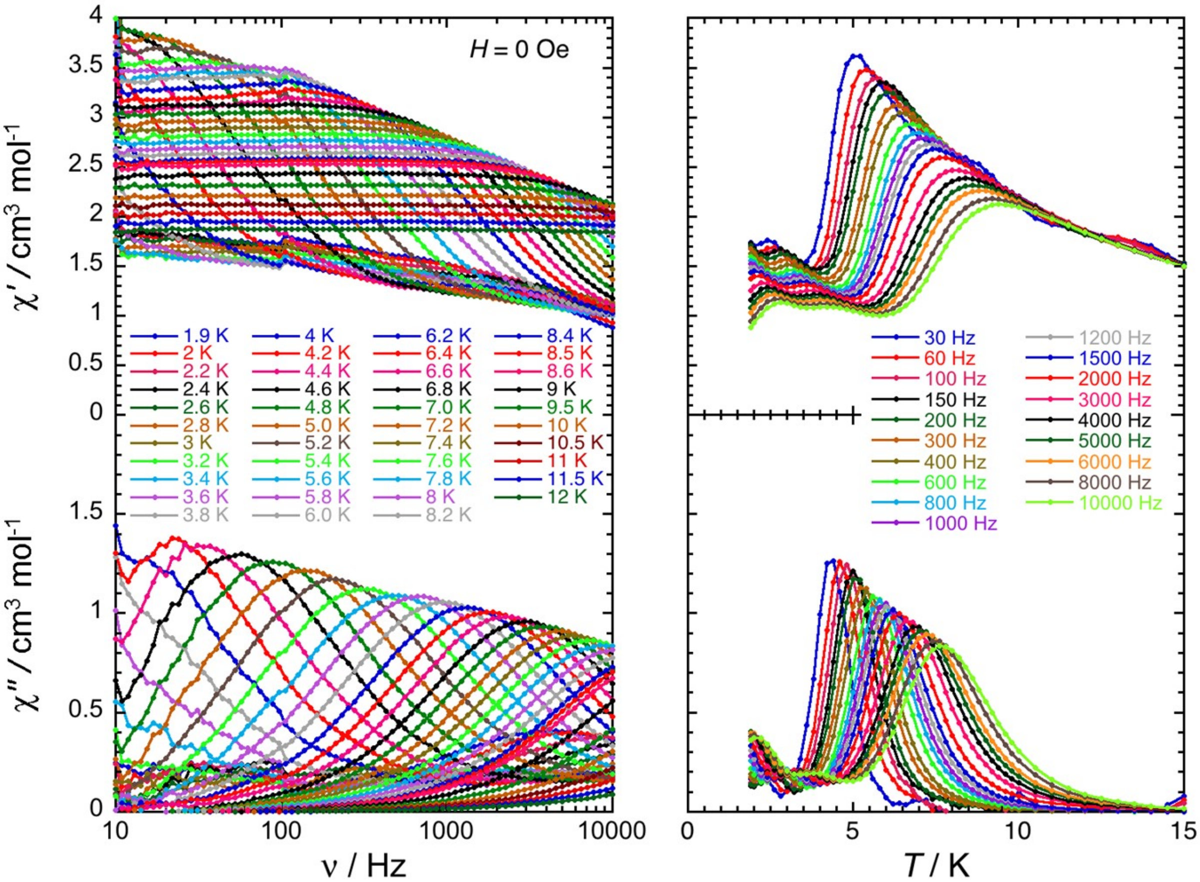

Fig. S4. ac frequency (left) and temperature (right) dependences of the real (χ', top) and imaginary (χ'', bottom) parts of the ac susceptibility for **1** in zero-dc field and for ac frequencies between 10 and 10000 Hz and between 1.9 and 12 K.

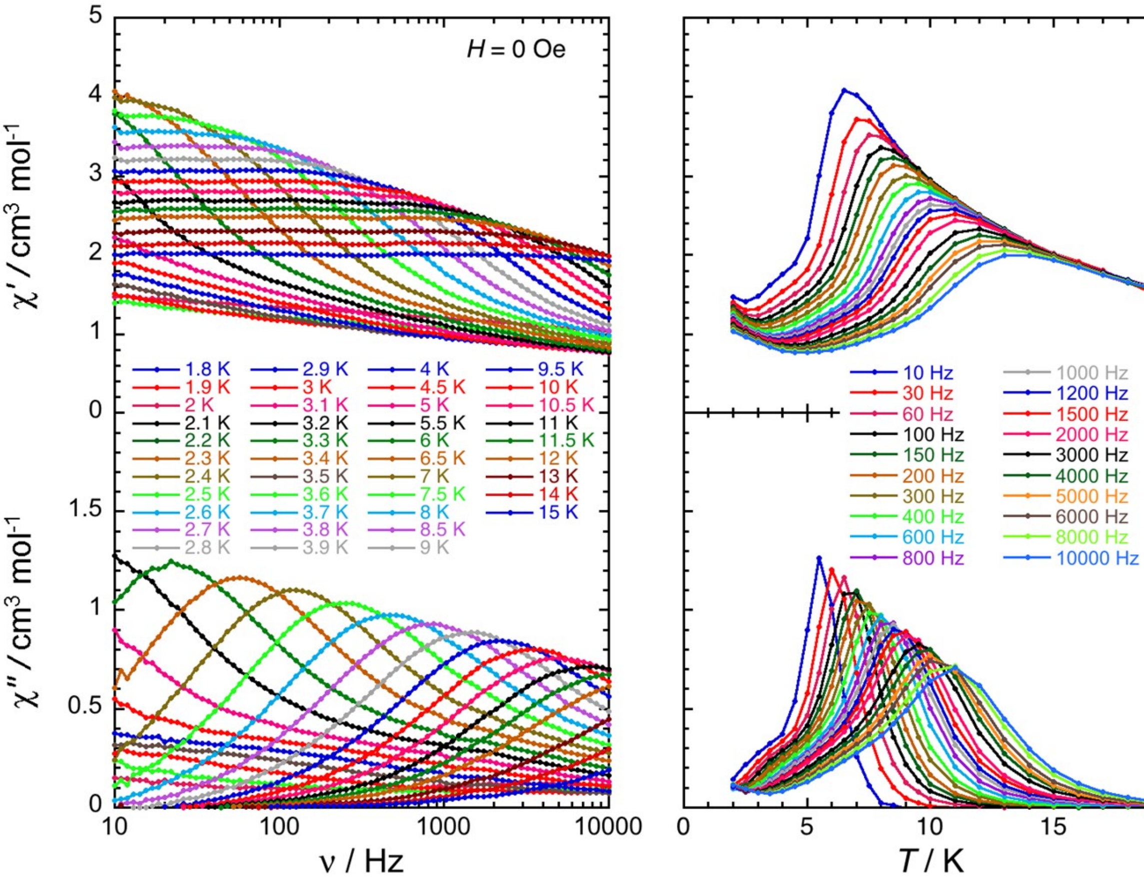

Fig. S5. ac frequency (left) and temperature (right) dependences of the real (χ', top) and imaginary (χ'', bottom) parts of the ac susceptibility for **2** in zero-dc field and for ac frequencies between 10 and 10000 Hz and between 1.8 and 15 K.

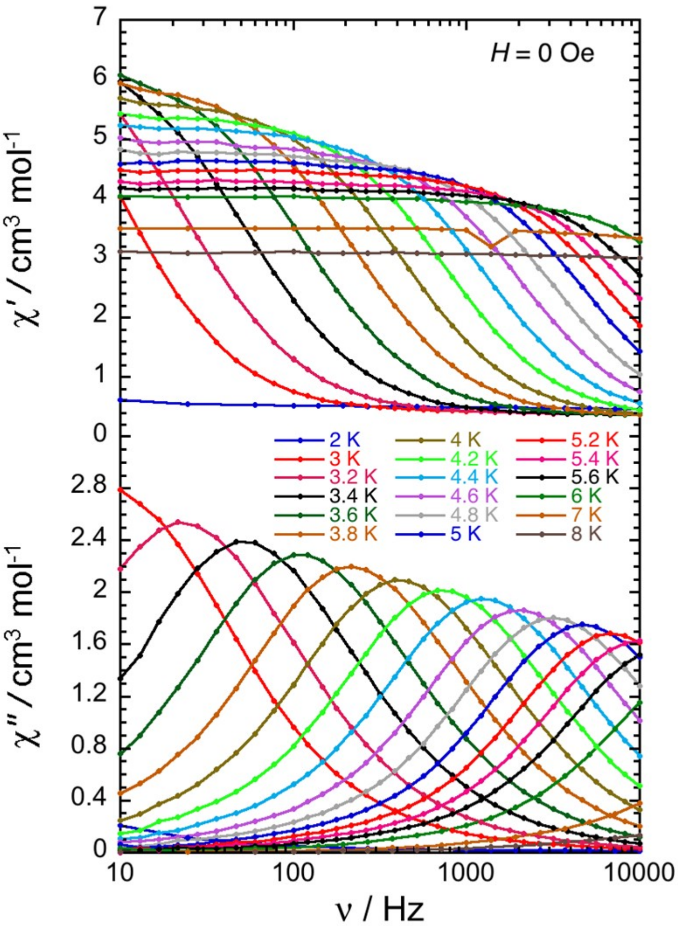

Fig. S6. ac frequency dependence of the real (χ', top) and imaginary (χ'', bottom) parts of the ac susceptibility for **3** in zero-dc field and for ac frequencies between 10 and 10000 Hz and between 2 and 8 K.

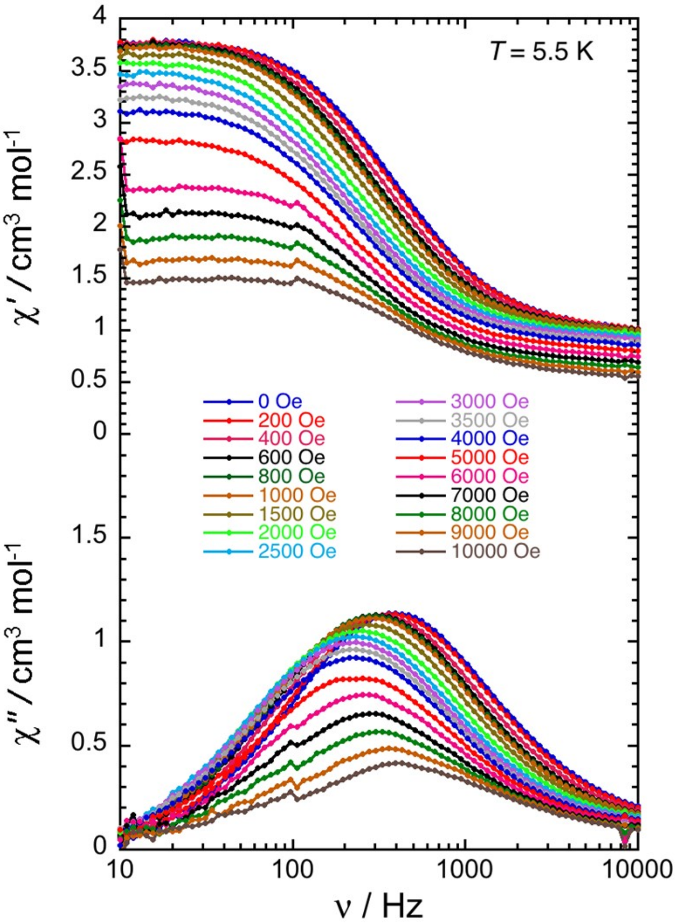

Fig. S7. ac frequency dependence of the real (χ', top) and imaginary (χ'', bottom) parts of the ac susceptibility for **1** at 5.5 K under different dc fields between 0 and 1 T and for ac frequencies between 10 and 10000 Hz.

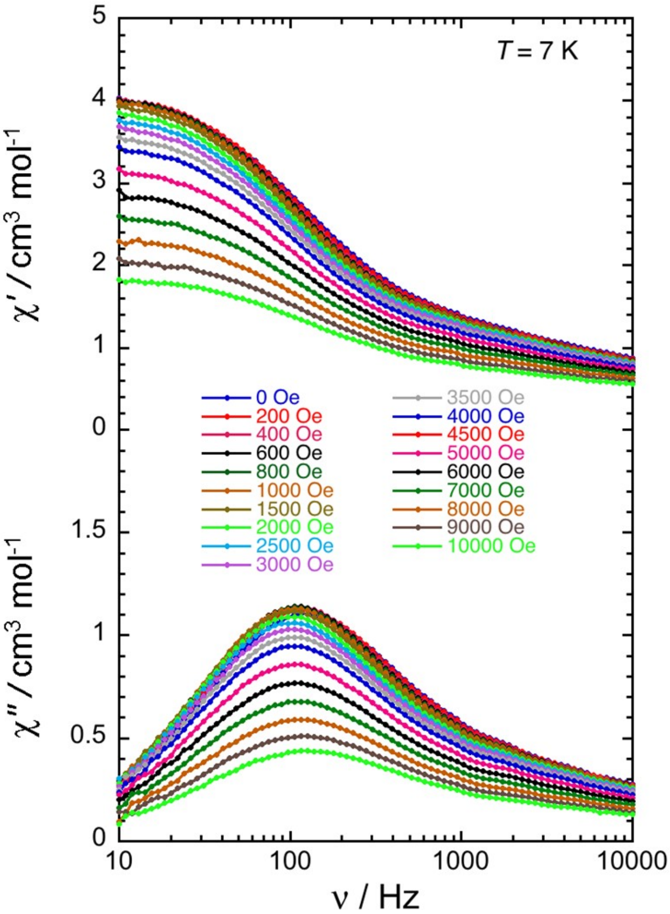

Fig. S8. ac frequency dependence of the real (χ', top) and imaginary (χ'', bottom) parts of the ac susceptibility for **2** at 7 K under different dc fields between 0 and 1 T and for ac frequencies between 10 and 10000 Hz.

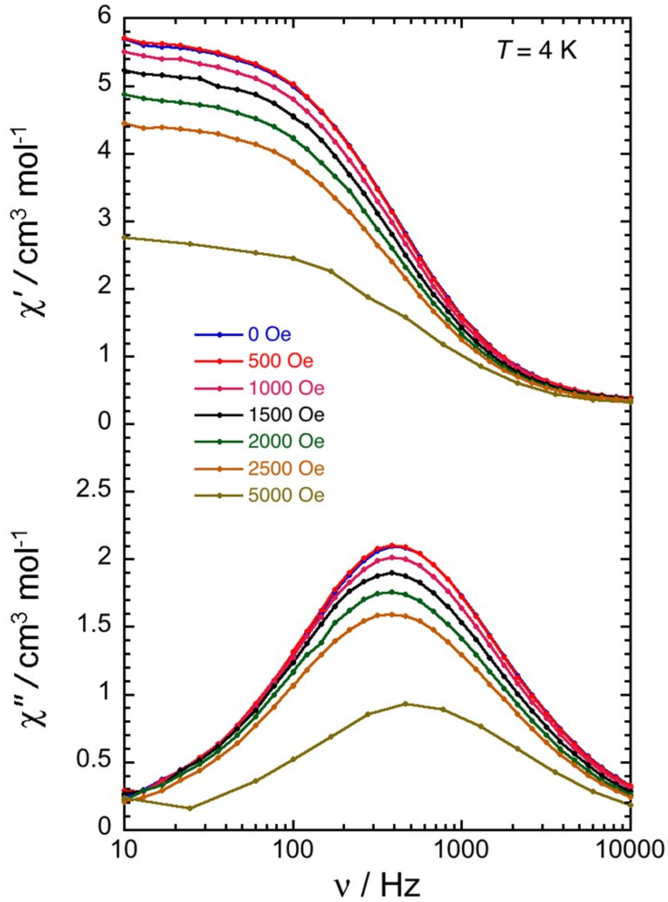

Fig. S9. ac frequency dependence of the real (χ', top) and imaginary (χ'', bottom) parts of the ac susceptibility for **3** at 4 K under different dc fields between 0 and 0.5 T and for ac frequencies between 10 and 10000 Hz.

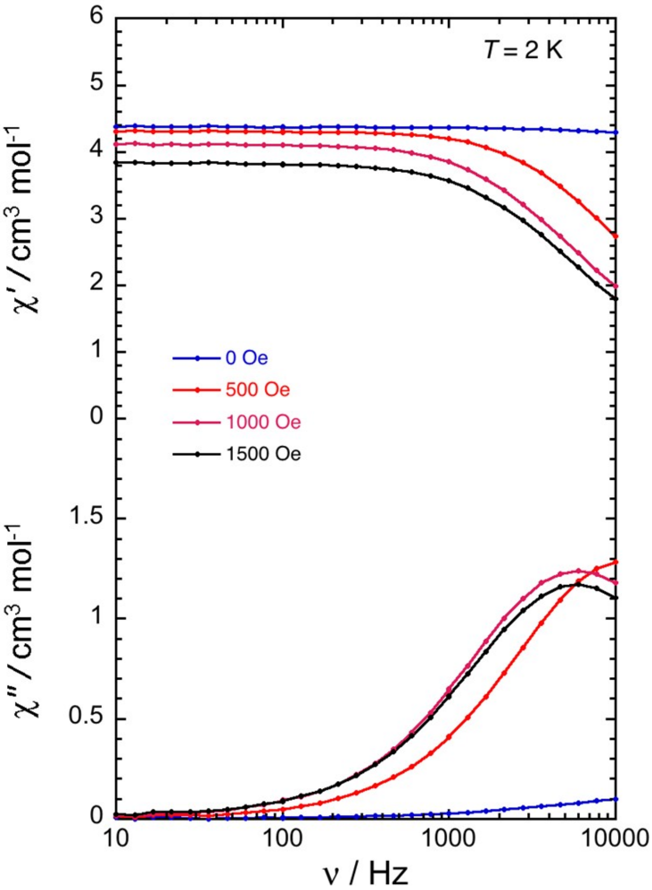

Fig. S10. ac frequency dependence of the real (χ', top) and imaginary (χ'', bottom) parts of the ac susceptibility for **4** at 2 K under different dc fields between 0 and 0.15 T and for ac frequencies between 10 and 10000 Hz.